NJC

Accepted Manuscript

This article can be cited before page numbers have been issued, to do this please use: J. Yan, C. Kang, Z. Bian, R. Jin, X. Ma and L. Gao, *New J. Chem.*, 2017, DOI: 10.1039/C7NJ02451G.

ROYAL SOCIETY OF CHEMISTRY

rsc.li/njc

View Article Online
DOI: 10.1039/C7NJ02451G

Journal Name

ARTICLE

Supramolecular self-assembly of chiral polyimides driven by repeat units and end groups

Received 00th January 20xx,
Accepted 00th January 20xx

DOI: 10.1039/x0xx00000x

www.rsc.org/

Jijun Yan,[a, b] Chuanqing Kang,*[a] Zheng Bian,[a] Rizhe Jin,[a] Xiaoye Ma[a] and Lianxun Gao[a]

Pyromellitic diimides (PMDIs) are effective building blocks for the construction of supramolecular systems but are infrequently used in comparison with other electron-deficient aromatic systems. We report PMDI-based chiral polyimides that form polymeric supramolecular systems with unique self-assembly features that show time-dependent spectroscopic behaviour. Extensive investigations revealed the driving forces for the self-assembly of the polyimides. One is the complementary aromatic π–π stacking between electron-accepting PMDI and electron-donating phenyl ring in the polymer backbones, and another is the hydrogen bonding interactions of the end groups. The self-assembly is readily disrupted by guest molecules with strong associations with the PMDI and the end groups. The introduction of flexible arylether diimides into the PMDI-based copolymer backbones and the sequence of PMDIs and arylether diimides in the copolymer backbones significantly influence the self-assembly of the polyimides. The results elucidate the mechanisms of polymeric self-assembly of chiral polyimides, providing important information for the development of materials based on polymeric supramolecular systems with properties and functions regulated by composition, sequence and end groups.

Introduction

Biological systems are extremely complicated but highly efficient. For example, spliceosome, a molecular machine assembled by snRNAs and protein complexes, has the capacity to selectively remove non-coding introns from transcribed pre-mRNAs with high accuracy and efficiency.[1] Most advanced biochemical functions are performed by controlling the precise self-assembly of chiral biomacromolecules and their resultant superstructures.[2] Some basic features of proteins can be mimicked by the self-assembly of synthetic foldamers.[3] However, unlike the vast majority of natural systems, synthetic polymeric supramolecular systems are typically constructed with achiral entities.

The introduction of chirality into the polymer-based supramolecular system not only imparts it with optical activity but can also may lead to unique hierarchical structures and advanced functions.[4-6] Furthermore, supramolecular systems based on chiral polymers are emerging as promising functional materials.[7-12] In recent years, M. Suginome et al have extensively studied the self-assembly of poly(quinoxaline-2, 3-diyl)s with tuneable main-chain helical sense, and these polymers have been applied in catalysis for organic conversions and as functional films in selectively reflecting or emission of circularly-polarised light.[13-20] Furthermore, I. Huc demonstrated an oligoamide that was able to encapsulate fructose with high selectivity through the formation of helical foldamer.[21] Importantly, the selective recognition of monosaccharides had been a challenge before the publication of that work. Consequently, the self-assembly of synthetic chiral polymers is expected to attract increasing research attention.

Non-covalent interactions, such as π–π interactions, hydrogen bonding and metal–ligand interactions, are common driving forces in the construction of polymeric supramolecular systems.[22] For example, complementary π–π stacking can endow a gel material with enhanced mechanical properties and facile self-healing characteristics,[23] and hydrogen bonding has been used to drive the association of small molecules or oligomers containing amide or urea groups to form supramolecular polyamide or polyurethane structures with rubber-like properties.[24, 25] However, as a class of polymer with excellent performance, polyimides have seldom been applied in the construction of supramolecular systems, despite the polymer typically having planar aromatic monomers that can act as π–donors or acceptors.[26] A limited number of functional polyimide-based supramolecular systems have been composed of structures that form hydrogen bonding or metal coordination,[27, 28] which bring additional complexity to the design and preparation of polymers. In addition, the excellent thermostability and chemical stability of polyimides can endow polyimide-based polymeric self-assembly with a wider application scope and prospects.

Several recent studies have demonstrated the self-assembly of small molecular pyromellitic diimide (PMDI) derivatives and

[a] State Key Laboratory of Polymer Physics and Chemistry, Changchun Institute of Applied Chemistry, Chinese Academy of Sciences, Changchun 130022, China. Email: kangcq@ciac.ac.cn.
[b] University of Chinese Academy of Sciences, Beijing 100049, China.
Electronic Supplementary Information (ESI) available: Synthesis of monomers and other small molecules, 1D and 2D NMR spectra, IR spectra, CD spectra and Job analyses. See DOI: 10.1039/x0xx00000x

View Article Online
DOI: 10.1039/C7NJ02451G

aromatic electron donors via charge-transfer π–π stacking.[29-32] The self-assembly of PMDI derivatives has been used to prepare unique supramolecular architectures with advanced functions, though they are used for construction of supramolecular systems much less frequently in comparison with other electron-deficient aromatic compounds such as naphthalenediimides.

Consequently, in the current study, we have investigated the self-assembly of PMDI-based chiral polymers, and polyimides with PMDIs and chiral centres in the main chain. Most recently, we presented a series of chiral polyimides derived from L-phenylalanine derivatives that showed slow self-assembly in dimethylsulfoxide (DMSO) to form gels and exhibited excellent performance in the recognition of enantiomers of chiral acids and weak Lewis basic anions.[33-35] Chiral polyimides containing PMDIs in the backbone have demonstrated unique sequence-dependence in self-assembly and molecular recognition.[35] We presumed that the complementary π–π interactions between the polymer chains result in the self-assembly, and the disturbance of the self-assembly by guest molecules was the intrinsic driving force for molecular recognition. We have, therefore, carried out extensive studies on the self-assembly of the chiral polyimide **PMDI-Phe** to gain deeper insight into how π–π stacking drives the self-assembly of chiral polyimide (Scheme 1). Chiroptical spectroscopy and NMR methods were used in this study. The contributions of the π–π stacking of the repeat units and the interactions of the end-groups to the polymeric self-assembly were investigated by performing comparative experiments using polyimides with different backbone compositions. Investigations into the association of the model molecules of the repeat units and end groups using a tweezer molecule confirmed the driving forces for the polymer self-assembly. Herein, we present the details of these studies. The results reveal the mechanism of the self-assembly of chiral polyimides and demonstrate a simple strategy for the design of chiral-polyimide-based supramolecular systems with tunable self-assembly behaviours.

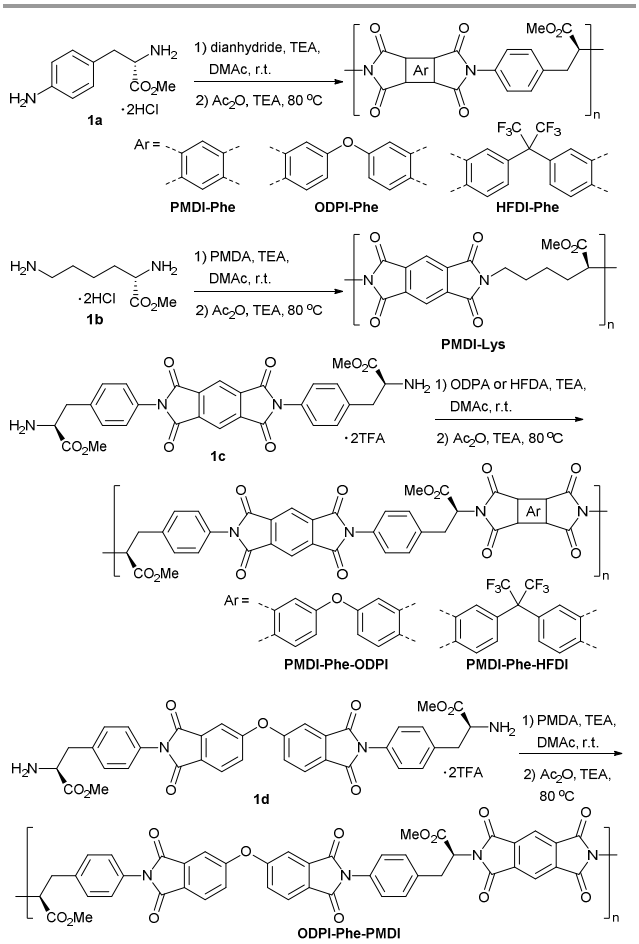

Scheme 1 Preparation of chiral polyimides. TEA = triethylamine, DMAc = *N,N*-dimethyl acetamide, PMDA = pyromellitic dianhydride, ODPA = 4,4'-oxydiphthalic anhydride, HFDA = 4,4'-(hexafluoroisopropylidene)diphthalic anhydride.

Experimental

Materials

All reagents were purchased from commercial resources and used without further purification unless specific stated. *N,N*-Dimethylacetamide (DMAc) was dried over CaH_2 and purified by distillation under reduce pressure prior to use. Pyromellitic dianhydride (PMDA), 4,4'-oxydiphthalic anhydride (ODPA) and 4,4'-(hexafluoroisopropylidene)diphthalic anhydride (HFDA) were purified by sublimation before use. External details on the synthesis of monomers, model molecules and the tweezer molecule were enclosed in the electronic supplementary information. Number-averaged molecular weights of the chiral polyimides were determined to be in range from 10,000 to 15,000 based on end group analysis with ^{1}H NMR.

Methods

^{1}H and ^{13}C NMR spectra were recorded at 25 °C using a Bruker AV300 or AV400 spectrometer with DMSO signal (δ_H = 2.50 ppm, δ_C = 39.52 ppm) as internal reference of chemical shifts. 2D NOESY experiments were carried out at a mixing time of 600 ms. Fourier transform infrared (FTIR) spectra were

View Article Online
DOI: 10.1039/C7NJ02451G

recorded on a Bruker Vertex70 Win-IR instrument. Specific rotations were measured on a Perkin Elmer 341LC polarimeter in a 1 dm tube cell. Circular dichroism (CD) spectra were recorded on a BioLogic MOS-450 spectrometer at 25 °C using a 0.1 mm cuvette (volume 60 µL, Starna Scientific Ltd). Alongside CD measurements, linear dichroism (LD) spectra were recorded to confirm that no LD contributions to CD signals (the LD intensities of all samples were very weak (<0.003) and completely negligible).

Unless otherwise specified, the concentration of the polymer used for all spectroscopic measurements was 5 mg/mL in DMSO. Polymer solution was prepared by dissolving pre-weighed amount of polymer in DMSO by heating in oil bath at 185 °C for 2 min. The first measurement was performed just after the newly-prepared polymer solution was cooled down to 25 °C within about 13 min. Time-dependent specific rotation and CD spectra were recorded at selected or random intervals. All samples in the cell or cuvette were stored in a constant temperature oven at 25 °C during the intervals of the time-dependent measurements to avoid the influence of temperature to the self-assembly of the polymers.

Polymerizations

All the polyimides were prepared through a similar procedure. Here presented the synthesis of **PMDI-Phe** as an example. To a completely dried 100-mL, three-necked flask equipped with a mechanical stirring device, were charged PMDA (0.692 g, 3.0 mmol), **1a** (0.654 g, 3.0 mmol), DMAc (18 mL) and TEA (0.45 mL, 3.2 mmol) under N_2 flow. The mixture was mechanically stirred at room temperature for 22h. Then TEA (0.45 mL, 3.2 mmol) and Ac_2O (0.90 mL, 6.4 mmol) was added to reaction solution and continued stirred for 1 h at room temperature and 2 h at 80°C. The resultant viscous suspension was poured into excess MeOH and filtrated to give pale yellow powder (0.95 g, 84.3%). Molecular weight 12550 Da. ^{1}H NMR (400 MHz, DMSO-d_6): 8.26 (s, 2H), 7.35 (s, 4H), 5.41 (s, 1H), 3.67 (s, 3H), 3.50-2.81 (m, 2H). ^{13}C NMR (101 MHz, DMSO-d_6): δ 168.58, 165.21, 165.06, 137.55, 136.89, 136.31, 135.70, 130.05, 129.38, 126.96, 118.72, 118.23, 117.70 , 52.92, 33.63. FT-IR (KBr): ν 1778 cm^{-1} (imide C = O, symmetrical stretching), 1716 cm^{-1} (imide C = O, asymmetrical stretching), 726 cm^{-1} (imide ring deformation) and 1380 cm^{-1} (C-N stretching).

ODPI-Phe. Not determined. Yield: 94.3%. ^{1}H NMR (300 MHz, DMSO-d_6): δ 8.09-7.82 (m, 2H), 7.69–7.39 (m, 4H), 7.38-7.13 (m, 4H), 5.32 (s, 1H), 3.78-3.61 (m, 3H), 3.55 (d, *J* = 10.7 Hz, 1H), 3.38 (d, *J* = 12.4 Hz, 1H). ^{13}C NMR (101 MHz, DMSO-d_6): δ 168.95, 166.24, 166.09, 165.91, 161.36, 160.84, 160.71, 160.19, 136.81, 134.32, 133.46, 130.31, 129.22, 126.98, 126.17, 125.95, 125.12, 124.80, 114.51, 114.30, 113.62, 113.45, 52.79, 52.52, 33.64. FT-IR (KBr): ν 1778 cm^{-1} (imide C = O, symmetrical stretching), 1716 cm^{-1} (imide C = O, asymmetrical stretching), 726 cm^{-1} (imide ring deformation) and 1380 cm^{-1} (C-N stretching).

HFDI-Phe. Not determined. Yield: 89.1%. ^{1}H NMR (300 MHz, DMSO-d_6): δ 8.16– 7.95 (m, 2H), 7.94–7.72 (m, 3H), 7.68 (d, *J* = 10.0 Hz, 1H), 7.35 (d, *J* = 8.3 Hz, 2H), 7.26 (d, *J* = 7.7 Hz, 2H), 5.35 (s, 1H), 3.67 (s, 3H), 3.56 (s, 1H), 3.35 (s, 1H). FT-IR (KBr): ν 1785 cm^{-1} (imide C = O, symmetrical stretching), 1726 cm^{-1} (imide C = O, asymmetrical stretching), 722 cm^{-1} (imide ring deformation) and 1380 cm^{-1} (C-N stretching).

PMDI-Lys. Not determined. Yield: 79.8%.^{1}H NMR (300 MHz, DMSO-d_6): δ 8.62–7.60 (m, 2H), 4.92 (s, 1H), 3.63 (s, 3H), 3.55 (s, 2H), 2.34-1.92 (m, 2H), 1.83-1.48 (m, 2H), 1.47-1.08 (m, 2H). ^{13}C NMR (101 MHz, DMSO-d_6): δ 165.41, 158.50, 158.19, 139.48, 137.11, 131.59, 127.56, 118.00, 49.67, 20.55. FT-IR (KBr): ν 1775 cm^{-1} (imide C = O, symmetrical stretching), 1719 cm^{-1} (imide C = O, asymmetrical stretching), 727 cm^{-1} (imide ring deformation) and 1388cm^{-1} (C-N stretching).

PMDI-Phe-ODPI. Molecular weight 10060 Da. Yield: 94.6%.^{1}H NMR (300 MHz, DMSO-d_6): δ 8.27 (s, 2H), 7.91 (d, *J* = 7.8 Hz, 2H), 7.71-7.47 (m, 4H), 7.34 (s, 8H), 5.34 (s, 2H), 3.69 (s, 6H), 3.58 (d, *J* = 12.5 Hz, 2H), 3.41 (d, *J* = 12.5 Hz, 2H). ^{13}C NMR (101 MHz, DMSO-d_6): δ 168.95, 166.21, 166.07, 165.29, 160.87, 137.11, 136.92, 133.46, 130.02, 129.30, 126.92, 126.18, 125.18, 117.74, 114.31, 52.81, 52.51, 33.67. FT-IR (KBr): ν 1778 cm^{-1} (imide C = O, symmetrical stretching), 1716 cm^{-1} (imide C = O, asymmetrical stretching), 726 cm^{-1} (imide ring deformation) and 1380 cm^{-1} (C-N stretching).

PMDI-Phe-HFDI. 15930 Da. Yield: 90.1%.^{1}H NMR (300 MHz, DMSO-d_6): δ 8.27 (s, 2H), 8.03 (d, *J* = 8.0 Hz, 2H), 7.93–7.63 (m, 4H), 7.35 (d, *J* = 6.5 Hz, 7H), 5.37 (s, 2H), 3.69 (s, 6H), 3.60 (d, *J* = 14.5 Hz, 2H), 3.40 (d, *J* = 14.5 Hz, 2H). ^{13}C NMR (101 MHz, DMSO-d_6): δ 168.77, 166.00, 165.93, 165.29, 137.75, 136.93, 131.85, 131.42, 130.04, 129.32, 126.95, 124.55, 123.87, 117.71, 52.84, 38.89, 33.71. FT-IR (KBr): ν 1746 cm^{-1} (imide C = O, symmetrical stretching), 1724 cm^{-1} (imide C = O, asymmetrical stretching), 722 cm^{-1} (imide ring deformation) and 1377 cm^{-1} (C-N stretching).

ODPI-Phe-PMDI. 15390 Da. Yield: 72.0%.^{1}H NMR (300 MHz, DMSO-d_6): δ 8.34-8.14 (m, 2H), 7.93 (d, *J* = 7.9 Hz, 2H), 7.67-7.41 (s, 4H), 7.40-7.03 (m, 8H), 5.37 (s, 2H), 3.86-3.64 (m, 6H), 3.64-3.49 (m, 2H), 3.48-3.23 (m, 2H). ^{13}C NMR (101 MHz, DMSO-d_6): δ 168.58, 166.03, 165.86, 165.09, 160.67, 136.72, 136.66, 136.31, 134.25, 130.35, 129.30, 126.98, 125.94, 124.83, 118.70, 113.57, 53.07, 52.90, 33.63. FT-IR (KBr): ν 1778 cm^{-1} (imide C = O, symmetrical stretching), 1716 cm^{-1} (imide C = O, asymmetrical stretching), 726 cm^{-1} (imide ring deformation) and 1380 cm^{-1} (C-N stretching).

Results and discussion

All polyimides were prepared by polycondensation of amino acid-derived diamines and dianhydrides followed by chemical imidisation with acetic anhydride and triethylamine (Scheme 1). **PMDI-Phe**, **ODPI-Phe** and **HFDI-Phe** were prepared from polycondensation of L-phenylalanine (Phe)-derived diamine **1a** with PMDA, ODPA and HFDA, respectively, whereas **PMDI-Lys** was prepared from methyl L-lysinate (**1b**) and PMDA. The asymmetric diamines **1a** and **1b** were arranged in random directions along the main chain. Copolymers **PMDI-Phe-ODPI** and **PMDI-Phe-HFDI** were prepared from diimide-derived diamine **1c** and ODPA and HFDA, respectively, whereas **ODPI-Phe-PMDI** was prepared from **1d** and PMDA. The methods used for the synthesis of the copolymers ensure well-defined

View Article Online
DOI: 10.1039/C7NJ02451G

chain structures. **PMDI-Phe-ODPI** and **ODPI-Phe-PMDI** have different diimide sequences based on the connection of PMDI to the aromatic or aliphatic carbon of the diamine monomer.

The PMDI-based chiral polyimide **PMDI-Phe** is capable of thermo-reversibly gelling DMSO during long-term standing.[32] Sustained dynamic changes of the specific rotations and circular dichroism (CD) spectra were observed during and after the gelation, strongly indicating the slow self-assembly of the polymer (Fig. 1a and 2a). In time-dependent CD spectra, the CD band at 272 nm changes from minimum negative to maximum positive within 170 hours (Fig. 2a). The phenomena may be derived from the formation of supramolecular chirality that is opposite to the initial chirality of the polymer chains before aggregation.[5, 36] The reverse of the chirality before and after self-assembly results in persistent changes in the time-dependent optical rotation and CD spectra. Subsequently, we tracked the time-dependent specific rotations of **PMDI-Phe** at different concentrations in DMSO. According to the tracking experiments, the variation range and rate of the CD spectra at 272 nm significantly decrease upon dilution of the polymer solution from 11.7 to 8.0 mM and below (Fig. 1b and Fig. S1), suggesting the dominative role of interchain stacking in the polymeric self-assembly.

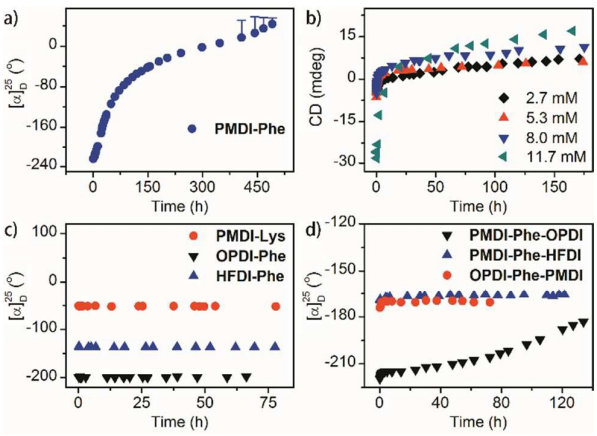

Fig. 1 Time-dependent specific rotations and CD spectra of chiral polyimides. a) Time-dependent specific rotation of **PMDI-Phe**; b) Plots of CD spectra of **PMDI-Phe** at 272 nm versus time at different concentrations in DMSO; c) Constant specific rotations of **PMDI-Lys**, **ODPI-Phe** and **HFDI-Phe**; d) Time-dependent specific rotations of copolyimides **PMDI-Phe-ODPI**, **ODPI-Phe-PMDI** and **HFDI-Phe-PMDI**.

Amino-acid-based polyimides have not shown the formation of polymeric supramolecular systems before.[26, 37] Therefore, we designed the chiral polyimides **PMDI-Lys**, **ODPI-Phe** and **HFDI-Phe** to distinguish the key structural factors that drive the polymeric self-assembly. Unlike the structure of **PMDI-Phe**, that of **PMDI-Lys** contains a long aliphatic chain. In **ODPI-Phe** and **HFDI-Phe**, the rigid and planar PMDI segment is replaced with flexible, non-planar 4,4'-oxydiphthalic diimide (ODPI) and 4,4'-(hexafluoroisopropylidene)diphthalic diimide (HFDI) segments. Notably, unlike **PMDI-Phe**, three new polyimides show constant specific rotations and CD spectra and no capability to induce gelation of DMSO (Fig. 1c and S2). The significant difference in chiroptical behaviour results from structural alterations, demonstrating the critical role of both PMDI and Phe segments in the slow self-assembly of **PMDI-Phe**. The results are in agreement with the presumption that the self-assembly of the chiral polyimide is driven by the complementary π–π stacking of planar PMDI segments and the phenyl ring of the Phe segments.[35]

Further investigation using the copolymers **PMDI-Phe-ODPI**, **PMDI-Phe-HFDI** and **ODPI-Phe-PMDI** confirmed the association of PMDI and Phe segments. In **PMDI-Phe-ODPI** and **PMDI-Phe-HFDI**, PMDI segments are connected to an aromatic carbon of the Phe segment; in **ODPI-Phe-PMDI**, the PMDI segments are conneted to an aliphatic carbon at the chiral centre. In comparison with **PMDI-Phe**, **PMDI-Phe-ODPI** shows less change in specific rotations and CD spectra with time, whereas the other two copolymers show almost constant specific rotations except for small changes in the initial stage within 2 hours (Fig. 1d and S3). Moreover, **PMDI-Phe-ODPI** gels DMSO after a longer period of standing compared to **PMDI-Phe**, while the other two copolymers do not gel DMSO at all. Therefore, the interactions between the PMDI and Phe segments are the key drivers for the slow stacking of the polymer chains, which can be suppressed to a certain degree by the introduction of flexible and non-planar ODPI and HFPI segments. Moreover, the subtle differences in the time-dependent specific rotations and gelation properties of **PMDI-Phe-ODPI** and **ODPI-Phe-PMDI** are probably a result of the different diimide sequences in the polymer backbones (Fig. 1d). The fact that the polyimide **PMDI-Phe-ODPI** displays more significant self-assembly than **ODPI-Phe-PMDI** indicates that the contributions to the polymeric self-assembly of the diaryl-substituted PMDI segments are more important than those of the dialkyl-substituted segments.[38]

The polymerisation of **PMDI-Phe** will leave a monoester of phthalic diacid (MPA) at one or both ends of the polymer chain upon quenching with methanol (Scheme 2). The end group MPA as a hydrogen bond donor and acceptor may influence the self-assembly of the polymer. However, the comparison between FT-IR spectra of the solution and gel of **PMDI-Phe** does not show clear evidence of hydrogen bonding or other intermolecular interactions (Fig. S4). Thus, the end-capped polyimide **PMDI-Phe-EC** was prepared to clarify the role of the MPA end group on the self-assembly of the polymer. The end-capped polyimide shows a negative Cotton signal at 256 nm, which slowly fades along with the formation of a positive Cotton signal at 282 nm; this is attributed to a longitudinally polarised imide transition (Fig. 2b).[39] In comparison with **PMDI-Phe**, **PMDI-Phe-EC** shows a similar but slower change of CD spectra at the specified wavelength with time and far slower gelation (Fig. 2c), indicating the important role of the end groups in the polymeric self-assembly. The time-dependent specific rotation of **PMDI-Phe-EC** gradually decreases linearly with time; this is a significantly different behaviour from that of **PMDI-Phe**, which is consistent with the trend in the later stages (Fig. 2d). This consistency suggests comparable or identical kinetics of self-assembly and resultant supramolecular architecture. In the time-dependent specific rotation of **PMDI-Phe**, the initial rapid stage is proposed to be

View Article Online
DOI: 10.1039/C7NJ02451G

a result of the synergistic effects of the interchain π–π stacking of PMDI and Phe segments and the hydrogen bonding from the MPA end groups, whereas the subsequent slow and steady stage is a result of π–π stacking alone.

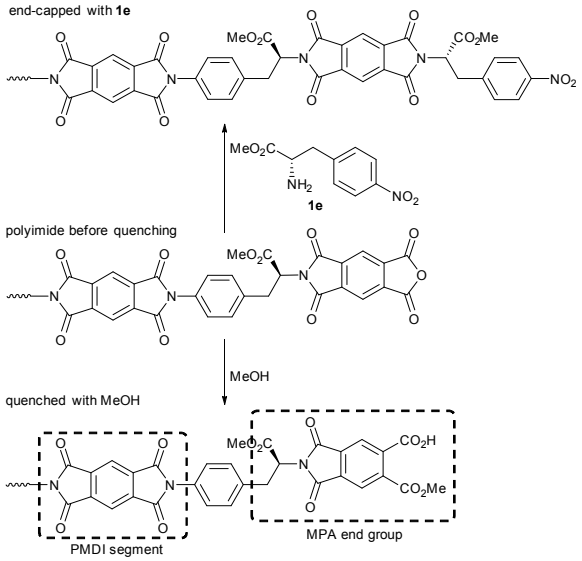

Scheme 2 Structure of the end group of **PMDI-Phe** and end-capped polymer

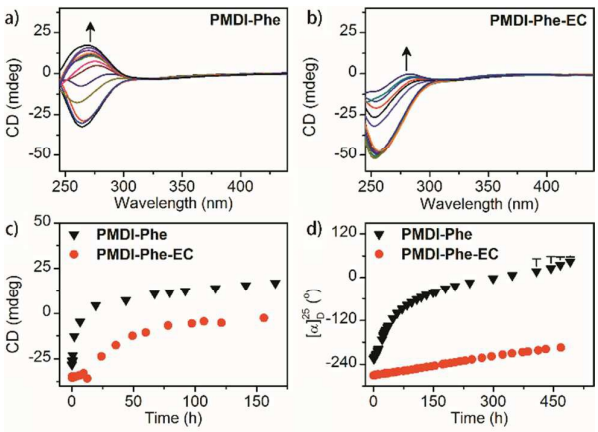

Fig. 2 Comparison of the chiroptical spectra of **PMDI-Phe** with and without end-capping. a) Time-dependent CD spectra of **PMDI-Phe**; b) Time-dependent CD spectra of **PMDI-Phe-EC**; c) Plots of the CD of **PMDI-Phe** and **PMDI-Phe-EC** at 272 nm versus time; d) Plots of specific rotations of **PMDI-Phe** and **PMDI-Phe-EC** versus time.

The interchain π–π stacking of PMDI and Phe segments was confirmed by NMR analysis. The 2D NOESY spectrum of **PMDI-Phe** in DMSO shows unambiguous cross peaks attributed to the short-range spatial coupling of H_a with H_b, H_c, H_d and H_e (Fig. 3a and 3b). H_a is located on the PMDI segment, and the others are located on the Phe segment. The results strongly suggest the short-range spatial proximity of the PMDI and Phe segments in the polymer backbones. Several naphthalenediimide-derived small molecules and polymers have been assembled through intermolecular π–π interactions, in which the electron-deficient diimides and electron-rich aryls are packed through their electrostatic complementation.[33, 40-42]

Consequently, the NOESY experiments confirm our assumption that the slow self-assembly of **PMDI-Phe** is driven by the complementary π–π interactions of the PMDI and Phe segments, similarly to other diimide molecules (Fig. 3c).

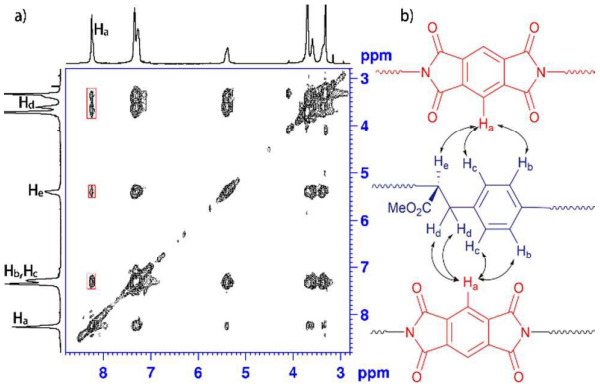

Fig. 3 NOESY spectra of **PMDI-Phe** (a) and interchain short-range spatial coupling of protons (b). Cross peaks in red rectangles in the NOESY spectra are derived from the spatial proximity of H_a in the PMDI segment and the protons of the Phe segment.

Since the π–π acceptor-donor interactions of the PMDI and Phe segments with the assistance of the hydrogen bonding of the end groups drive the self-assembly of **PMDI-Phe**, a guest molecule with a stronger affinity for the PMDI segments or the end groups will inhibit the polymeric self-assembly. Previously, we utilised similar tactics in molecular recognition, in which the original self-assembly process of polyimides was disturbed by guest anions and chiral acids.[33-35] Recent reports have demonstrated the recognition of pyromellitic diimide through complementary π–π stacking and hydrogen-bondings using a pyrenyl-based tweezer molecule.[43, 44] Hence, we designed the novel isophthalic diamide-based tweezer **IPDA** to investigate the inhibition of the self-assembly (Scheme 3). As expected, the time-dependent specific rotation of **PMDI-Phe** is constant in the presence of **IPDA** (Fig. 4a). The introduction of **IPDA** into **PMDI-Phe** also leads to invariable CD spectrum with significant decrease of the intensity of CD band at 272 nm (Fig. S5), which is attributed to the destruction of both original polymer conformation and supramolecular architectures. An enhanced absorption at 305 nm in UV-Vis spectra is observed along with the colour change from light yellow to deep red (Fig. S6). Thus, the competitive association of **IPDA** with the PMDI segments and MPA end groups prevents the original interactions between the polymer backbones.

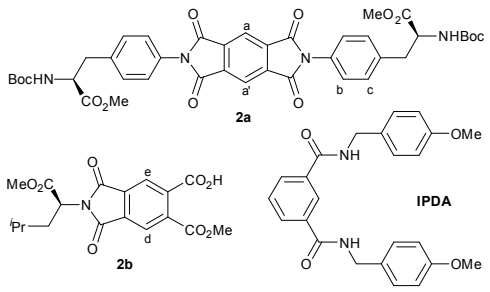

Scheme 3 Models of PMDI segment and end group and tweezer molecule.

View Article Online
DOI: 10.1039/C7NJ02451G

Accordingly, we prepared compounds **2a** and **2b** as models for the repeat unit and end group of **PMDI-Phe**, respectively (Scheme 3). The interactions between **IPDA** and **PMDI-Phe** were simulated with the model compounds. The introduction of **IPDA** into a solution of **2a** leads to a colour change from light yellow to deep red in the same way as introduction of **IPDA** into a solution of **PMDI-Phe**, as a result of a charge-transfer absorption from the diimide-tweezer's π–π stacking.[45] Hydrogen bonding between the amides of **IPDA** and carbonyl of **2a** are also driving forces for the association.[43, 44] The ^{1}H NMR spectrum of **2a** becomes complicated owing to association with **IPDA**, which breaks the symmetric microenvironment of **2a** (Fig. 4b). The proton signal at 8.36 ppm (H_a of **2a**) shifts upward to 7.39 ppm, and the signals for two protons on the Phe aryls at 7.42 ppm (protons H_b and H_c) split into two signals at 7.64 and 7.20 ppm (Fig. 4b). These changes result from differences in the chemical microenvironment of the protons because of the shielding and deshielding effect exerted by **IPDA**, which leads to downshifting and upshifting of the originally overlapping proton signals. A mixture of **2b** and **IPDA** exhibits upshifts of the signals for H_d and H_e in **2b** from 8.18 and 8.15 ppm to 8.09 and 7.90 ppm, respectively, owing to shielding from **IPDA** (Fig. 4c). Job analyses based on the ^{1}H NMR spectra for the complexations of both **2a** and **2b** with **IPDA** clearly show a preference for 1:1 binding, and the binding constants were determined to be 60.0 and 115.9 M^{-1} (Fig. S7-10). The binding tests demonstrated that **IPDA** is capable of binding with not only the PMDI segment but also the end group, which is the essential factor for inhibiting the polymeric self-assembly.

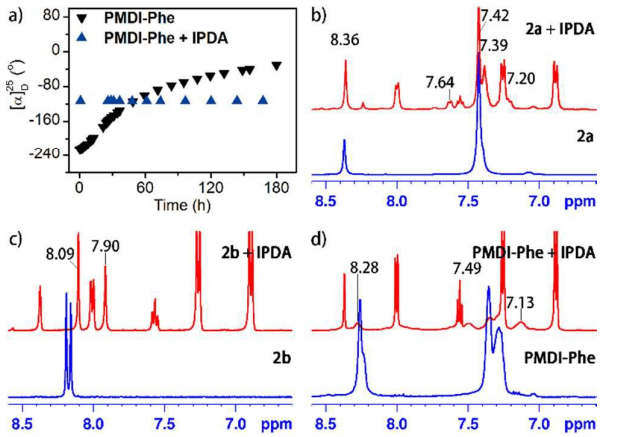

Fig. 4 Inhibition of the polymeric self-assembly of **PMDI-Phe** and simulations with model compounds. a) Time-dependent specific rotation of PMDI-Phe in the absence and presence of tweezer molecules; b), c) and d) ^{1}H NMR spectra (regional) of **2a**, **2b** and **PMDI-Phe**, respectively, in the absence (bottom) and presence (top) of **IPDA**. One of the H_a protons of **2a** overlaps with a proton of **IPDA** at 8.36 ppm according to the integration.

^{1}H NMR analysis of a mixture of **IPDA** and **PMDI-Phe** revealed similar splits and upshifts of the proton signals with the appearance of new peaks at 8.02 (overlapped with the protons of **IPDA**), 7.49 and 7.13 ppm, suggesting similar interactions of the polymer with **IPDA** to those of the models (Fig. 4d). Moreover, the NOESY spectra of the mixture does not show the original cross peaks of the PMDI proton H_a with the Phe protons corresponding to the interchain interactions of **PMDI-Phe** as shown in the NOESY spectra of the polymer itself (Fig. 3a and 5a), suggesting that **IPDA** prevents the interactions of the polymer backbones. Through the complementary π–π stacking and hydrogen bonding, the backbones of **PMDI-Phe** are entangled to form micelles that are responsible for the gelation (Fig. 5b). However, in the presence of **IPDA**, the backbones are thought to be embedded in the tweezer molecule to form necklace-like chains with local sandwich structures at the repeat units and end groups, which disrupt the associations of the polymer chains (Fig. 5b). The destruction of the original micelle networks results in sol-gel conversion, whereas each of the 'necklaces' is free in DMSO.

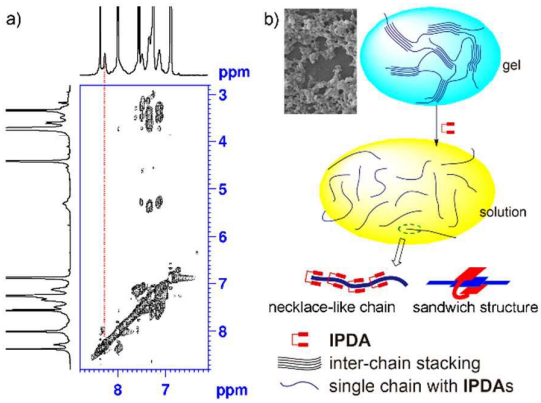

Fig. 5 NOESY spectra (regional) of a mixture of **PMDI-Phe** and **IPDA** (a) and a schematic illustration of the inhibition of the self-assembly of **PMDI-Phe** by **IPDA** (b).

It is remarkable that the integration of multiple PMDI and Phe segments in **PMDI-Phe** afford the capacity to self-assemble, while the model of the repeat unit, **2a**, does not show the capability to self-assemble. Thus, these investigations also provide potential techniques for the regulation or amplification of polymer properties and their potential functions through the integration of building blocks to obtain group effects in the polymeric self-assembly. As we have described above, the properties of the polyimide with rigid and planar aromatic diimides and Phe segments are also regulated by the introduction of flexible and non-planar structures, which changes the original interactions. Another remarkable phenomenon is the spectroscopic difference between **PMDI-Phe-OPDI** and **OPDI-Phe-PMDI**, which reveals the importance of defined sequence for the polymeric self-assembly.[13-15, 35] We also found the influence of the end groups upon the self-assembly of **PMDI-Phe**, which may present a tactic to manipulate the self-assembly or other properties of the polymer.[46, 47] According to these results, the rationale design of compositions, sequences and even end groups may be effective strategies for regulating the properties and functions of supramolecular systems and materials based on chiral polyimides.

View Article Online
DOI: 10.1039/C7NJ02451G

Conclusions

We conducted a deep investigation into the mechanism of the self-assembly of **PMDI-Phe** through comparative studies and spectroscopic analyses. Our study revealed that the formation of the polymeric supramolecular system is driven by the complementary π–π stacking between the repeat units (the PMDI and Phe segments) and the hydrogen bonding between the MPA end groups. The presence of both interactions in the self-assembly of the polyimide results in two-stage kinetics in the chiroptical spectra. The study demonstrates a strategy for regulating polymeric self-assembly behaviours by exploiting concerted π–π interactions and hydrogen bonding as well as introducing flexible or planar structures that stay out of the direct interactions of polymer backbones. Further development of functional materials based on the knowledge obtained in this study is currently in progress in our laboratory and will be reported in due course.

Acknowledgements

This work was financially supported by the National Natural Science Foundation of China (21574126 and 21274142) and the National Basic Research Program of China (2014CB643603).

Notes and references

1 S. W. Stevens, D. E. Ryan, H. Y. Ge, R. E. Moore, M. K. Young, T. D. Lee and J. Abelson, *Mol. Cell*, 2002, **9**, 31-44.
2 G. Gunkel-Grabole, S. Sigg, M. Lomora, S. Lorcher, C. G. Palivan and W. P. Meier, *Biomat. Sci.*, 2015, **3**, 25-40.
3 S. Erbas-Cakmak, D. A. Leigh, C. T. McTernan and A. L. Nussbaumer, *Chem. Rev.*, 2015, **115**, 10081-10206.
4 H. K. Bisoyl, Q. Li, *Angew. Chem. Int. Ed.*, 2016, **55**, 2994-3010.
5 M. Liu, L. Zhang, T. Wang, *Chem. Rev.*, 2015, **115**, 7304-7397.
6 E. Yashima, K. Maeda, H. Lida, Y. Furusho, K. Nagai, *Chem. Rev.*, 2009, **109**, 6102-6211.
7 Y. Zhao, N. A. A. Rahirn, Y. J. Xia, M. Fujiki, B. Song, Z. B. Zhang, W. Zhang and X. L. Zhu, *Macromolecules*, 2016, **49**, 3214-3221.
8 G. Fukuhara, *Polym. J.*, 2015, **47**, 649-655.
9 E. A. Appel, J. del Barrio, X. J. Loh and O. A. Scherman, *Chem. Soc. Rev.*, 2012, **41**, 6195-6214.
10 M. Burnworth, L. Tang, J. R. Kumpfer, A. J. Duncan, F. L. Beyer, G. L. Fiore, S. J. Rowan and C. Weder, *Nature*, 2011, **472**, 334-337.
11 R. Vaiyapuri, B. W. Greenland, H. M. Colquhoun, J. M. Elliott and W. Hayes, *Polym. Int.*, 2014, **63**, 933-942.
12 L. Ma, C. J. Zhou, Q. Z. Yang, X. G. Yang, C. Zhang and L. Q. Liao, *Curr. Org. Chem.*, 2014, **18**, 1937-1947.
13 Y. Nagata, M. Uno and M. Suginome, *Angew. Chem. Int. Ed.*, 2016, **55**, 7126-7130.
14 Y. Nagata, T. Nishikawa and M. Suginome, *ACS Macro Lett.*, 2016, **5**, 519-522.
15 Y. Nagata, R. Takeda and M. Suginome, *Chem. Commun.*, 2015, **51**, 11182-11185.
16 Y. Nagata, T. Nishikawa and M. Suginome, *J. Am. Chem. Soc.*, 2015, **137**, 4070-4073.
17 Y. Z. Ke, Y. Nagata, T. Yamada and M. Suginome, *Angew. Chem. Int. Ed.*, 2015, **54**, 9333-9337.
18 Y. Akai, L. Konnert, T. Yamamoto and M. Suginome, *Chem. Commun.*, 2015, **51**, 7211-7214.
19 T. Yamamoto, Y. Akai and M. Suginome, *Angew. Chem. Int. Ed.*, 2014, **53**, 12785-12788.
20 Y. Nagata, T. Nishikawa and M. Suginome, *Chem. Commun.*, 2014, **50**, 9951-9953.
21 N. Chandramouli, Y. Ferrand, G. Lautrette, B. Kauffmann, C. D. Mackereth, M. Laguerre, D. Dubreuil and I. Huc, *Nat. Chem.*, 2015, **7**, 334-341.
22 C. Rest, R. Kandanelli and G. Fernandez, *Chem. Soc. Rev.*, 2015, **44**, 2543-2572.
23 S. Burattini, H. M. Colquhoun, J. D. Fox, D. Friedmann, B. W. Greenland, P. J. Harris, W. Hayes, M. E. Mackay and S. J. Rowan, *Chem. Commun.*, 2009, 6717-6719.
24 P. Cordier, F. Tournilhac, C. Soulie-Ziakovic and L. Leibler, *Nature*, 2008, **451**, 977-980.
25 Y. J. Kim, P. H. Huh and B. K. Kim, *J. Polym. Sci. B Polym. Phys.*, 2015, **53**, 468-474.
26 D.-J. Liaw, K.-L. Wang, Y.-C. Huang, K.-R. Lee, J.-Y. Lai and C.-S. Ha, *Prog. Polym. Sci.*, 2012, **37**, 907-974.
27 E. Schab-Balcerzak, J. Konieczkowska, M. Siwy, A. Sobolewska, M. Wojtowicz and M. Wiacek, *Opt. Mater.*, 2014, **36**, 892-902.
28 E. Schab-Balcerzak, H. Flakus, A. Jarczyk-Jedryka, J. Konieczkowska, M. Siwy, K. Bijak, A. Sobolewska and J. Stumpe, *Opt. Mater.*, 2015, **47**, 501-511.
29 C. Musumeci, M. Wałęsa-Chorab, A. Gorczyński, G. Markiewicz, A. Bogucki, R. Świetlik, Z. Hnatejko, W. Jankowski, M. Hoffmann, E. Orgiu, A. R. Stefankiewicz, V. Patroniak, A. Ciesielski and P. Samorì, *ACS Omega*, 2017, **2**, 1672-1678.
30 S. B. Krishnan and K. R. Gopidas, *Chem. Eur. J.*, 2017, **23**, 9600-9606.
31 H. M. Colquhoun, Z. Zhu, D. J. Williams, M. G. B. Drew, C. J. Cardin, Y. Gan, A. G. Crawford and T. B. Marder, *Chem. Eur. J.*, 2010, **16**, 907-918.
32 P. Jana, S. Maity, S. K. Maity, P. K. Ghorai and D. Haldar, *CrystEngComm*, 2012, **14**, 6586-6592.
33 J. Yan, C. Kang, Z. Bian, X. Ma, R. Jin, Z. Du, L. Gao, *Chem. Eur. J.*, 2017, **23**, 5824-5829.
34 J. Yan, C. Kang, X. Ma, Z. Du, Z. Bian, R. Jin, L. Gao, *Asian J. Org. Chem.*, 2017, DOI: 10.1002/ajoc.201700333.
35 J. Yan, C. Kang, Z. Bian, R. Jin, X. Ma, Z. Du, H. Yao, *Chem. Asian J.*, 2017, **12**, 841-845.
36 P. Duan, Y. Li, L. Li, J. Deng, M. Liu, *J. Phys. Chem. B*, 2011, **115**, 3322-3329.
37 C. Kang, J. Yan and L. Gao, *Prog. Chem.*, 2015, **27**, 59-69.
38 H. M. Colquhoun, Z. Zhu, C. J. Cardin, Y. Gan and M. G. Drew, *J. Am. Chem. Soc.*, 2007, **129**, 16163-16174.
39 J. Gawroński, M. Brzostowska, K. Gawrońska, J. Koput, U. Rychlewska, P. Skowronek and B. Nordén, *Chem. Eur. J.*, 2002, **8**, 2484-2494.
40 M. B. Avinash and T. Govindaraju, *Adv. Funct. Mater.*, 2011, **21**, 3875-3882.
41 P. Jana, S. K. Maity, S. Bera, R. K. Ghorai and D. Haldar, *CrystEngComm*, 2013, **15**, 2512-2518.
42 M. B. Avinash, P. K. Samanta, K. V. Sandeepa, S. K. Pati and T. Govindaraju, *Eur. J. Org. Chem.*, 2013, 5838-5847.
43 H. M. Colquhoun, Z. Zhu, C. J. Cardin, Y. Gan and M. G. B. Drew, *J. Am. Chem. Soc.*, 2007, **129**, 16163-16174.
44 Z. Zhu, C. J. Cardin, Y. Gan and H. M. Colquhoun, *Nat. Chem.*, 2010, **2**, 653-660.
45 H. M. Colquhoun and Z. X. Zhu, *Angew. Chem. Int. Ed.*, 2004, **43**, 5040-5045.
46 H. Sawada, *J. Fluorine Chem.*, 2003, **121**, 111-130.
47 T. Shanmugam, C. Sivakumar and A. S. Nasar, *J. Polym. Sci. Polym. Chem.*, 2008, **46**, 5414-5430.

View Article Online
DOI: 10.1039/C7NJ02451G

Complementary aromatic π–π stacking and hydrogen bonding induce time-dependent chiroptical spectroscopic behaviours of L-phenylalaninate-derived chiral polyimide.